Available online at www.sciencedirect.com

Thermochimica Acta 402 (2003) 183–191

thermochimica acta

www.elsevier.com/locate/tca

Low-temperature heat capacity and thermodynamic properties of $[Re_2(Ile)_4(H_2O)_8](ClO_4)_6$ (Re = Nd, Er, Ile = isoleucine)

Xiaozheng Lan, Zhi-Cheng Tan*, Beiping Liu, Zhaodong Nan, Lixian Sun, Fen Xu

Thermochemistry Laboratory, Dalian Institute of Chemical Physics, Chinese Academy of Sciences, Dalian 116023, China

Received 13 September 2002; received in revised form 30 September 2002; accepted 28 November 2002

Abstract

The heat capacities of two kinds of rare-earth element solid complexes with isoleucine $[Re_2(Ile)_4(H_2O)_8](ClO_4)_6$ (where Re = Nd, Er, and Ile = isoleucine) have been measured by an automatic adiabatic calorimeter in the temperature range from 80 to 370 K. Two solid–solid phase transitions were found from the C_p curve of Nd formed complex in the range of 165–175 K with a peak temperature of 167.88 K and in the range of 195–210 K with a peak temperature of 202.13 K. The corresponding molar enthalpies of these phase transitions were determined to be 404.61 J mol^{-1} and 2.955 kJ mol^{-1}, respectively. One solid–solid phase transition was found for the Er formed complex in the range of 190–205 K with a peak temperature of 193.42 K. The corresponding molar enthalpy of this transition was 14.11 kJ mol^{-1}. Smooth heat capacities and thermodynamic functions relative to the standard state (298.15 K), $H_T - H_{298.15}$, $S_T - S_{298.15}$ and $-[G_T - G_{298.15}]$, of the two compounds, were calculated on basis of experimental heat capacity data. Possible mechanisms of thermal decompositions for the pair of compounds were suggested according to the thermogravimetric (TG) analysis.

Keywords: Rare-earth complex; Isoleucine; $[Nd_2(Ile)_4(H_2O)_8](ClO_4)_6$; $[Er_2(Ile)_4(H_2O)_8](ClO_4)_6$; Heat capacity; Thermal stability; TG analysis

1. Introduction

Rare-earth elements have found their applications in many areas nowadays because of their unique properties: used as the main components of permanent magnet, catalysts, glass ceramics and so on [1]. In recent years, they are also used as micro fertilizer, pesticide [2] and antibacterial agent [3]. Accompanying these applications, rare-earth elements are inevitably spread into food chain, biological chain and then into the bodies of human beings. This leads people to care about and study the influence and the long-term effect of rare-earth elements on themselves [4]. Rare-earth complex formed with amino acid were then synthesized for this purpose, because amino acid is the basic unit comprising protein and enzyme, the functional materials in the body of human beings. In the last 20 years, nearly 200 kinds of these complexes have been synthesized, and about 50 kinds have their own crystallograms [5]. As we know, only with thermodynamic data we can quantitatively describe their properties of energetics, e.g., thermal stability and stable forms in different temperature range, melting point and energy changing in different processes and so on. Comparisons of thermodynamic data of a series of complexes comprised by the same Re (or ligands) with different ligands (or Re) may make us to get deeper understanding of their properties.

---

* Corresponding author. Tel.: +86-411-4379215;
fax: +86-411-4691570.
E-mail address: tzc@dicp.ac.cn (Z.-C. Tan).

doi:10.1016/S0040-6031(02)00573-7

In this paper, we report the low-temperature heat capacities of two complexes $[Nd_2(Ile)_4(H_2O)_8](ClO_4)_6$ and $[Er_2(Ile)_4(H_2O)_8](ClO_4)_6$ in the range 80–370 K. The possible mechanism of thermal decomposition of the two compounds is analysed by TG experiments.

2. Experimental

2.1. Sample synthesis and characterization

$[Re_2(Ile)_4(H_2O)_8](ClO_4)_6$ (Re = Nd, Er) were synthesized by use of the procedure reported earlier [6]: rare-earth oxides (Er_2O_3, Nd_2O_3, purity 99.9%) were dissolved in perchloric acid to get the aqueous solution of the rare-earth perchlorates. Then isoleucine was added into the solution with the molar ratio of 2:1 with rare-earth element at pH = 4–5. The crystalline product was obtained by slow evaporation of the solvent at room temperature. After washing with water, followed by air-drying, the composition of these crystals was determined by elemental analysis.

The purities of the crystals were found to be more than 99.90% by EDTA titrimetric analysis.

2.2. Adiabatic calorimeter

Heat capacity measurements were performed with a high-precision automatic adiabatic calorimeter on the basis of the Nernst stepwise heating method [7]. The calorimeter mainly comprises a sample cell, an adiabatic/inner shield, a guard/outer shield, a platinum resistance thermometer, an electric heater, two sets of chromel–copel thermocouples and a high vacuum can. The sample cell is made of gold-plated copper with an inner volume of about 6 cm^3. Four gold-plated copper vanes of 0.2 mm thickness are placed in the cell in order to promote heat transfer between the cell and the sample. The platinum resistance thermometer was inserted into the copper sheet soldered at the bottom of the sample cell. The heating wire was wound bifilarly on the outer surface of the cell. The lid of the cell with a ca 5 cm long copper capillary was sealed to the sample cell with epoxy resin after the sample was put in it. The air in the cell was drained out by a vacuum pump and replaced with helium (0.1 MPa) in order to enhance the heat transfer from the cell to the sample during the heating period. Then the capillary was pinched off and soldered at the end. Pressure of the evacuated can was kept less than 1×10^{-3} Pa during experiment

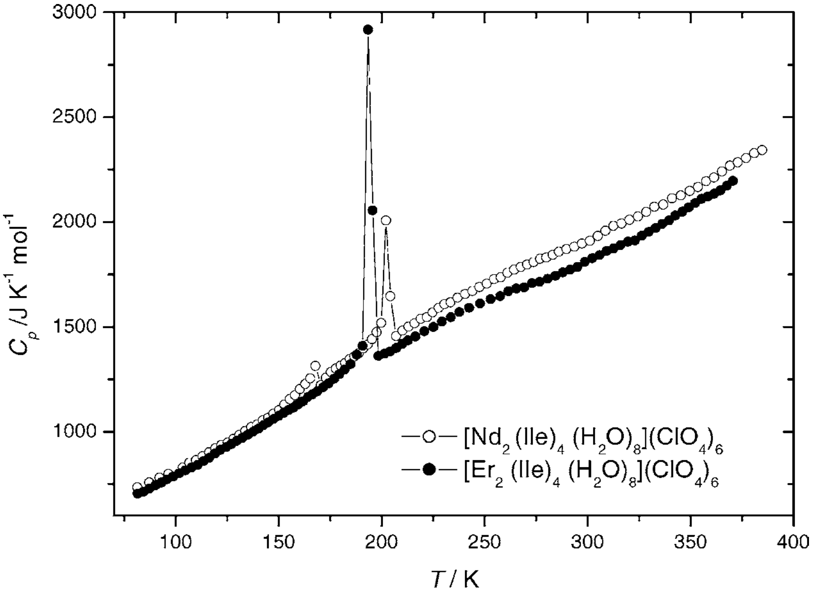

Fig. 1. The curve of experimental molar heat capacity of $[Re_2(Ile)_4(H_2O)_8](ClO_4)_6$ (Re = Nd, Er, Ile = isoleucine).

process to eliminate the heat leakage due to gas convection. Liquid nitrogen was used as the coolant for the vacuum can. One set of chromel–copel thermocouples was put to detect the temperature differences between the sample cell and the inner shield and the other one for the inner and outer shields, which ensures the temperature difference between them being controlled within less than 0.5 mK. The sample cell was heated by the standard discrete heating method. The temperature increment during a heating period was kept 2–4 K, and the temperature drift was maintained at about $10^{-3}\,K\,min^{-1}$ during the equilibrium period. All the data were automatically collected by using a Data Acquisition/Switch Unit (Model: 34970 A, Agilent, USA) and processed by a microcomputer.

The mass of $[Nd_2(Ile)_4(H_2O)_8](ClO_4)_6$ and $[Er_2(Ile)_4(H_2O)_8](ClO_4)_6$ used for heat capacity measurements was 2.8380 g (1.77 mmol) and 2.1179 g (1.36 mmol), respectively.

Calibration of the adiabatic calorimeter was performed with standard material α-Al_2O_3 (1.6382 g, 0.016 mol). Deviations of the measured heat capacity of α-Al_2O_3 from the recommended values of the former National Bureau of Standards (NBSs) [8] were within ±0.2% in the range from 80 to 400 K.

2.3. Thermal analysis

Thermogravimetric (TG) tests (setsys 16/18, SETARAM, France) were done under nitrogen (99.999%

Table 1
The experimental molar heat capacity of $[Nd_2(Ile)_4(H_2O)_8](ClO_4)_6$ ($M = 1554.00\,g\,mol^{-1}$)

T (K)	$C_{p,m}$ ($J\,mol^{-1}\,K^{-1}$)	T (K)	$C_{p,m}$ ($J\,mol^{-1}\,K^{-1}$)	T (K)	$C_{p,m}$ ($J\,mol^{-1}\,K^{-1}$)
81.494	734.82	180.125	1313.80	270.744	1796.54
87.263	757.92	182.409	1327.66	273.876	1808.08
92.271	781.02	184.641	1346.14	276.965	1824.25
96.529	797.76	186.839	1358.19	280.020	1830.41
103.460	829.52	189.016	1375.39	283.098	1842.73
106.765	851.08	191.180	1396.23	286.182	1856.59
109.998	863.02	193.323	1415.21	289.652	1870.45
113.156	882.23	195.448	1440.16	293.500	1882.00
116.260	900.27	197.547	1474.64	297.334	1896.29
119.311	920.37	199.832	1517.80	301.168	1910.20
122.307	936.54	202.127	2006.89	304.960	1932.35
125.268	947.32	204.347	1645.61	308.724	1958.84
128.177	965.80	207.059	1456.94	312.604	1980.12
131.046	984.28	210.080	1481.36	316.565	1991.32
133.868	1002.38	213.085	1499.23	320.472	2010.57
136.705	1022.00	216.062	1516.34	324.441	2025.20
139.504	1033.52	219.013	1538.13	328.390	2047.60
142.226	1053.84	221.946	1546.43	332.424	2071.39
144.959	1065.89	224.853	1569.41	336.683	2081.40
147.617	1085.48	227.746	1590.97	341.071	2112.20
150.244	1103.14	230.602	1607.91	345.349	2126.06
152.835	1129.09	233.556	1617.15	349.518	2148.39
155.396	1155.87	236.897	1638.70	353.587	2166.86
157.936	1173.68	240.512	1655.72	357.588	2193.81
160.441	1203.78	244.098	1670.27	361.498	2211.52
162.930	1226.52	247.630	1689.52	365.350	2240.78
165.414	1253.13	251.088	1705.69	369.197	2267.72
167.878	1312.50	254.501	1725.70	373.056	2284.66
170.517	1222.06	257.843	1735.86	376.937	2303.39
173.019	1256.06	261.116	1757.27	380.832	2327.63
175.434	1284.54	264.373	1771.13	384.747	2341.58
177.791	1299.94	267.574	1784.99		

pure) atmosphere with a flow rate of 20 ml min^{-1} and heating rate of 10 K min^{-1}. The mass of the samples for the tests were 2.8 and 3.4 mg for $[Nd_2(Ile)_4(H_2O)_8](ClO_4)_6$ and $[Er_2(Ile)_4(H_2O)_8](ClO_4)_6$, respectively.

3. Results and discussion

3.1. Heat capacity

The low-temperature experimental molar heat capacities of $[Nd_2(Ile)_4(H_2O)_8](ClO_4)_6$ are shown in Fig. 1 and listed in Table 1. The result is fitted as the function of reduced temperature (X) using the least square fitting method and obtained the following polynomials:

$$T = 81.494\text{–}165.414\,\mathrm{K},$$

$$C_{p,\mathrm{m}}\ (\mathrm{J\,K^{-1}\,mol^{-1}}) = 940.32 + 236.27X + 16.375X^2 + 9.2004X^3 + 39.223X^4 + 14.794X^5$$

where $X = (T - 123.454)/41.96$ and T is the absolute temperature. The linear regression coefficient $R^2 = 0.9996$

$$T = 170.517\text{–}190.547\,\mathrm{K},$$

$$C_{p,\mathrm{m}}\ (\mathrm{J\,K^{-1}\,mol^{-1}}) = 1340.8 + 83.281X + 8.0666X^2 + 41.942X^3$$

where $X = (T - 184.0325)/13.515$, $R^2 = 0.9992$

Table 2
The experimental molar heat capacity for $[Er_2(Ile)_4(H_2O)_8](ClO_4)_6$ ($M = 1600.0431\ \mathrm{g\,mol^{-1}}$)

T (K)	$C_{p,\mathrm{m}}$ ($\mathrm{J\,mol^{-1}\,K^{-1}}$)	T (K)	$C_{p,\mathrm{m}}$ ($\mathrm{J\,mol^{-1}\,K^{-1}}$)	T (K)	$C_{p,\mathrm{m}}$ ($\mathrm{J\,mol^{-1}\,K^{-1}}$)
81.616	704.4	164.259	1165.01	269.281	1688.11
84.520	713.64	166.553	1177.39	273.086	1707.66
87.447	728.48	169.041	1193.36	276.881	1713.91
90.294	744.12	171.722	1211.23	280.641	1728.83
93.076	757.56	174.373	1229.55	284.361	1743.11
95.793	771.01	176.994	1252.37	288.030	1758.14
98.695	784.99	179.587	1273.43	291.635	1772.73
101.783	800.54	182.148	1295.95	295.194	1785.83
104.801	815.74	184.935	1322.48	298.755	1808.81
107.761	828.74	187.948	1367.73	302.314	1827.83
110.661	842.05	190.920	1407.88	305.846	1841.91
113.511	859.28	193.416	2917.31	309.327	1860.64
116.316	876.21	195.716	2054.62	312.780	1874.11
119.080	894.95	198.422	1360.05	316.208	1889.02
121.806	911.71	201.369	1371.79	319.586	1904.72
124.513	925.51	204.294	1382.97	322.996	1912.34
127.213	940.86	207.195	1397.95	326.366	1934.77
129.877	956.09	210.074	1420.12	329.709	1951.73
132.508	971.81	212.927	1435.05	333.025	1970.57
135.108	985.72	216.541	1453.99	336.307	1990.78
137.677	998.71	220.904	1478.17	339.558	2007.13
140.215	1014.52	225.215	1498.85	342.781	2029.89
142.728	1030.91	229.461	1524.43	345.983	2048.86
145.213	1044.61	233.669	1545.90	349.150	2068.61
147.671	1060.51	237.813	1570.81	352.283	2089.85
150.105	1075.31	242.520	1591.16	355.385	2110.24
152.516	1088.93	247.812	1610.38	358.465	2121.56
154.904	1102.84	253.066	1631.11	361.517	2135.91
157.274	1113.96	257.638	1645.41	364.546	2150.93
159.628	1129.51	261.566	1668.48	367.551	2172.48
161.955	1144.93	265.444	1682.41	370.532	2196.25

Table 3
Smooth heat capacity and thermodynamic functions of $[Nd_2(Ile)_4\ (H_2O)_8](ClO_4)_6$ ($M = 1554.00\,g\,mol^{-1}$)

T (K)	$C_{p,m}$ ($J\,mol^{-1}\,K^{-1}$)	$H_T - H_{298.15}$ ($kJ\,mol^{-1}$)	$S_T - S_{298.15}$ ($J\,mol^{-1}\,K^{-1}$)	$-[G_T - G_{298.15}]$ ($kJ\,mol^{-1}$)
80	730.47	−235.83	−1499.11	115.90
85	748.57	−234.48	−1454.30	110.87
90	768.77	−233.04	−1410.95	106.06
95	790.93	−231.49	−1368.80	101.46
100	814.79	−229.83	−1327.63	97.07
105	840.02	−228.05	−1287.27	92.88
110	866.31	−226.13	−1247.58	88.90
115	893.37	−224.08	−1208.48	85.11
120	920.98	−221.90	−1169.87	81.51
125	949.05	−219.57	−1131.71	78.11
130	977.64	−217.11	−1093.94	74.90
135	1007.01	−214.50	−1056.49	71.87
140	1037.69	−211.74	−1019.32	69.03
145	1070.46	−208.82	−982.35	66.38
150	1106.46	−205.73	−945.46	63.91
155	1147.20	−202.45	−908.53	61.63
160	1194.59	−198.95	−871.37	59.53
165	1251.02	−195.19	−833.78	57.62
167.878	Maximum			
175	1276.22	−188.85	−795.75	49.59
180	1315.55	−182.36	−759.22	45.70
185	1346.82	−175.71	−722.73	42.00
190	1382.75	−168.89	−686.36	38.48
195	1436.10	−161.85	−649.81	35.14
202.127	Maximum			
210	1476.84	−150.88	−595.62	25.80
215	1510.99	−143.41	−560.45	22.91
220	1543.01	−135.77	−525.36	20.19
225	1573.13	−127.98	−490.37	17.65
230	1601.56	−120.04	−455.50	15.28
235	1628.48	−111.97	−420.79	13.08
240	1654.10	−103.76	−386.25	11.06
245	1678.59	−95.43	−351.90	9.21
250	1702.13	−86.98	−317.75	7.54
255	1724.87	−78.41	−283.81	6.04
260	1746.98	−69.73	−250.09	4.71
265	1768.58	−60.94	−216.59	3.54
270	1789.83	−52.04	−183.31	2.55
275	1810.83	−43.04	−150.26	1.72
280	1831.72	−33.94	−117.43	1.06
285	1852.59	−24.72	−84.81	0.55
290	1873.54	−15.41	−52.40	0.21
295	1894.66	−5.99	−20.19	0.03
298.15	1898.50	0.00	0.00	0.00
300	1916.03	3.54	11.83	0.01
305	1937.73	13.17	43.67	0.15
310	1959.80	22.92	75.34	0.44
315	1982.30	32.77	106.86	0.89
320	2005.28	42.74	138.24	1.50
325	2028.76	52.82	169.49	2.26
330	2052.78	63.03	200.63	3.18
335	2077.33	73.35	231.67	4.26
340	2102.44	83.80	262.62	5.49

Table 3 (*Continued*)

T (K)	$C_{p,\mathrm{m}}$ (J mol^{-1} K^{-1})	$H_T - H_{298.15}$ (kJ mol^{-1})	$S_T - S_{298.15}$ (J mol^{-1} K^{-1})	$-[G_\mathrm{T} - G_{298.15}]$ (kJ mol^{-1})
345	2128.10	94.38	293.49	6.88
350	2154.28	105.08	324.30	8.42
355	2180.98	115.92	355.06	10.12
360	2208.15	126.89	385.77	11.98
365	2235.76	138.00	416.44	14.00
370	2263.76	149.25	447.06	16.16
375	2292.09	160.64	477.65	18.48
380	2320.68	172.17	508.20	20.94

Table 4
Smooth heat capacity and thermodynamic functions of $[Er_2(Ile)_4(H_2O)_8](ClO_4)_6$ ($M = 1600.0431$ g mol^{-1})

T (K)	$C_{p,\mathrm{m}}$ (J mol^{-1} K^{-1})	$H_T - H_{298.15}$ (kJ mol^{-1})	$S_T - S_{298.15}$ (J mol^{-1} K^{-1})	$-[G_T - G_{298.15}]$ (kJ mol^{-1})
80	693.17	−280.37	−1526.43	158.26
85	718.58	−276.84	−1483.60	150.73
90	742.63	−273.19	−1441.87	143.42
95	766.40	−269.41	−1401.11	136.31
100	790.63	−265.52	−1361.19	129.40
105	815.75	−261.51	−1322.01	122.70
110	841.99	−257.36	−1283.44	116.18
115	869.33	−253.08	−1245.39	109.86
120	897.64	−248.67	−1207.79	103.73
125	926.69	−244.11	−1170.55	97.79
130	956.19	−239.40	−1133.63	92.03
135	985.87	−234.54	−1097.00	86.45
140	1015.48	−229.54	−1060.62	81.05
145	1044.90	−224.39	−1024.49	75.84
150	1074.15	−219.09	−988.57	70.81
155	1103.45	−213.65	−952.88	65.95
160	1133.26	−208.06	−917.37	61.28
165	1164.33	−202.31	−882.01	56.78
170	1197.78	−196.41	−846.76	52.46
175	1235.10	−190.33	−811.51	48.32
180	1278.24	−184.05	−776.13	44.35
185	1329.63	−177.53	−740.44	40.55
190	1392.26	−170.73	−704.18	36.94
193.416	Maximum			
205	1388.55	−150.34	−599.85	27.37
210	1418.71	−143.32	−566.02	24.45
215	1447.77	−136.15	−532.30	21.71
220	1475.63	−128.84	−498.69	19.13
225	1502.23	−121.40	−465.24	16.72
230	1527.58	−113.82	−431.94	14.47
235	1551.69	−106.12	−398.84	12.40
240	1574.64	−98.31	−365.93	10.48
245	1596.52	−90.38	−333.24	8.73
250	1617.45	−82.34	−300.78	7.15
255	1637.58	−74.20	−268.55	5.72
260	1657.06	−65.97	−236.56	4.46
265	1676.06	−57.63	−204.81	3.36
270	1694.78	−49.21	−173.30	2.42

Table 4 (*Continued*)

T (K)	$C_{p,\mathrm{m}}$ (J mol^{-1} K^{-1})	$H_T - H_{298.15}$ (kJ mol^{-1})	$S_T - S_{298.15}$ (J mol^{-1} K^{-1})	$-[G_T - G_{298.15}]$ (kJ mol^{-1})
275	1713.39	−40.69	−142.03	1.63
280	1732.09	−32.07	−110.98	1.00
285	1751.05	−23.37	−80.15	0.52
290	1770.46	−14.56	−49.52	0.20
295	1790.47	−5.66	−19.09	0.03
298.15	1803.45	0.00	0.00	0.00
300	1811.23	3.34	11.18	0.01
305	1832.88	12.45	41.29	0.14
310	1855.50	21.67	71.27	0.42
315	1879.17	31.01	101.14	0.85
320	1903.94	40.47	130.92	1.43
325	1929.79	50.05	160.63	2.15
330	1956.69	59.77	190.29	3.03
335	1984.55	69.62	219.92	4.05
340	2013.23	79.61	249.53	5.23
345	2042.54	89.75	279.14	6.55
350	2072.23	100.04	308.75	8.02
355	2101.98	110.48	338.36	9.64
360	2131.40	121.06	367.98	11.41
365	2160.06	131.79	397.58	13.33
370	2187.40	142.66	427.15	15.39

$$T = 207.059\text{–}384.747\,\mathrm{K},$$

$$C_{p,\mathrm{m}}(\mathrm{J\,K^{-1}\,mol^{-1}}) = 1898.5 + 378.15X + 41.653X^2 + 68.004X^3 - 38.322X^4$$

where $X = (T - 295.91)/88.85$, $R^2 = 0.9997$

The heat capacity of $[\mathrm{Er_2(Ile)_4(H_2O)_8}](\mathrm{ClO4})_6$ is shown in Fig. 1 and listed in Table 2 and the fitting result is as follows:

$$T = 83.5\text{–}187.95\,\mathrm{K},$$

$$C_{p,\mathrm{m}}(\mathrm{J\,K^{-1}\,mol^{-1}}) = 989.64 + 310.47X + 2.331X^2 - 38.589X^3 + 41.556X^4 + 57.027X^5 + 1.5928X^6$$

where $X = (T - 135.73)/52.23$, T is absolute temperature, $R^2 = 0.9999$

$$T = 198.42\text{–}370.53\,K,$$

$$C_{p,\mathrm{m}}(\mathrm{J\,K^{-1}\,mol^{-1}}) = 1737.3 + 332.9X + 204.06X^2 + 129.75X^3 - 390.52X^4 - 40.225X^5 + 230.76X^6$$

where $X = (T - 284.48)/86.06$, $R^2 = 0.9991$

The heat capacity curve of $[\mathrm{Nd_2(Ile)_4(H_2O)_8}]$-$(\mathrm{ClO_4})_6$ in Fig. 1 presents two endothermal peak at 167.88 and 202.13 K. Also there is one endothermal peak at 193.24 K in the curve of heat capacity of $[\mathrm{Er_2(Ile)_4(H_2O)_8}](\mathrm{ClO_4})_6$. As the melting points of them are much higher than these temperatures, the peaks indicate the solid–solid phase transitions of the two complexes. In other temperature range, the curve of the heat capacity is smooth, which show the stable forms of the two compounds.

3.2. *The molar enthalpy and entropy of solid–solid phase transition*

Molar enthalpy $\Delta_{\mathrm{trs}}H_{\mathrm{m}}$ and entropy $\Delta_{\mathrm{trs}}S_{\mathrm{m}}$ of solid–solid phase transition can be calculated from the $C_{p,\mathrm{m}}(T)$ curves by using the following equations:

$$\Delta_{\mathrm{trs}}H_{\mathrm{m}} = \frac{Q - n\int_{T_{\mathrm{i}}}^{T_{\mathrm{trs}}} C_{p(\mathrm{i})}\,\mathrm{d}T - n\int_{T_{\mathrm{trs}}}^{T_{\mathrm{f}}} C_{p(\mathrm{f})}\,\mathrm{d}T - n\int_{T_{\mathrm{i}}}^{T_{\mathrm{f}}} H_0\,\mathrm{d}T}{n},$$

$$\Delta_{\mathrm{trs}}S_{\mathrm{m}} = \frac{\Delta_{\mathrm{trs}}H}{T_{\mathrm{trs}}}$$

where T_{trs} is the temperature at which the solid–solid phase transition takes place, T_{i} the temperature a few degrees lower than the initial phase transition temperature, T_{f} is a temperature slightly higher than the final

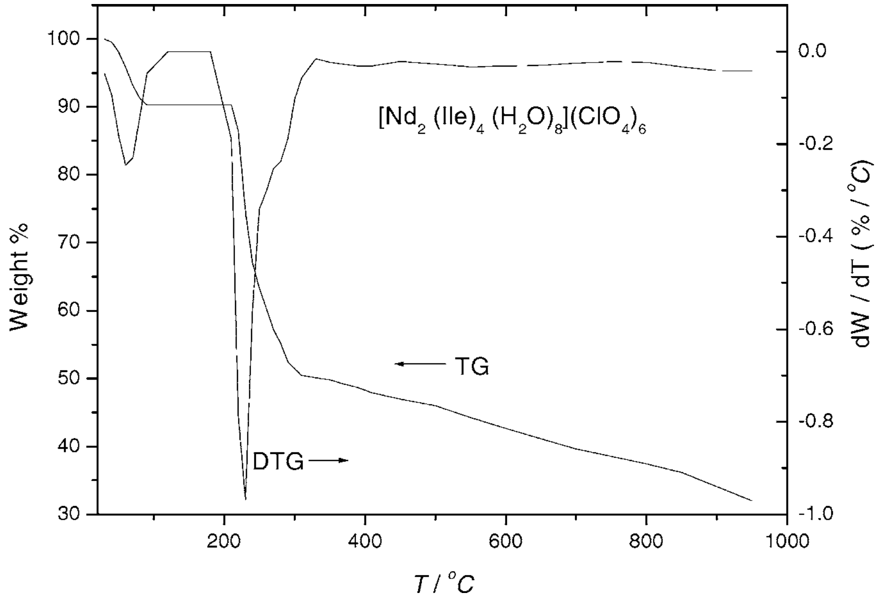

Fig. 2. TG curve of rare-earth complex with isoleucine [$Nd_2(Ile)_4(H_2O)_8](ClO_4)_6$.

phase transition temperature, Q is the total energy provided for the sample cell from T_i to T_f, H_0 is the heat capacity of the empty sample cell (from T_i to T_f), $C_{p(i)}$ the heat capacity of the sample in the lower temperature range from T_i to T_{trs}, $C_{p(f)}$ the heat capacity of the sample in the higher temperature range from T_{trs} to T_f, and n is molar amount of the sample. The molar enthalpy and molar entropy of the phase transition

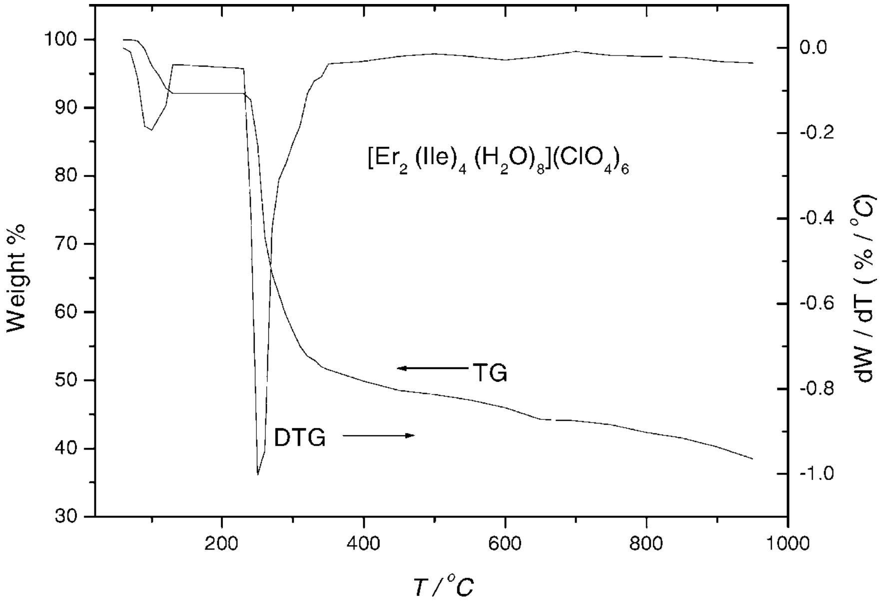

Fig. 3. TG curve of rare-earth complex with isoleucine [$Er_2(Ile)_4(H_2O)_8](ClO_4)_6$.

are thus obtained

$[Nd_2(Ile)_4(H_2O)_8](ClO_4)_6$:

$\Delta_{trs}H_m = 404.61\,J\,mol^{-1}$,

$\Delta_{trs}S_m = 2.41\,J\,K^{-1}\,mol^{-1}$ at 167.88 K,

$\Delta_{trs}H_m = 2.955\,kJ\,mol^{-1}$,

$\Delta_{trs}S_m = 14.62\,J\,K^{-1}\,mol^{-1}$ at 202.13 K,

$[Er_2(Ile)_4(H_2O)_8](ClO_4)_6$:

$\Delta_{trs}H_m = 14.11\,kJ\,mol^{-1}$,

$\Delta_{trs}S_m = 72.95\,J\,K^{-1}\,mol^{-1}$ at 193.42 K

4. Thermodynamic functions

On the basis of the above experimental heat capacity of the complexes, smooth values of the $C_{p,m}$ can be obtained from the polynomials with respect to the reduced temperature $X = (T - T_1)/T_2$, where $T_1 = (T_h + T_l)/2$, $T_2 = (T_h - T_l)/2$, T_h and T_l are the highest and the lowest temperature in the range where the polynomials are valid. Thermodynamic functions in relative to the standard state (298.15 K), $H_T - H_{298.15}$, $S_T - S_{298.15}$ and $-[G_T - G_{298.15}]$, were calculated on the basis of the polynomials with the following formulas:

$$H_T - H_{298.15} = \int_{298.15}^{T} C_{p,m}\,dT,$$

$$S_T - S_{298.15} = \int_{298.15}^{T} \frac{C_{p,m}}{T}\,dT$$

$$-[G_T - G_{298.15}] = T\int_{298.15}^{T} \frac{C_{p,m}}{T}\,dT - \int_{298.15}^{T} C_{p,m}\,dT$$

The values of the above functions are actually the sum of integrity in different temperature range plus the value changed during the phase transition. All the data are listed in Tables 3 and 4.

4.1. *TG analysis and the mechanism of thermal decomposition*

TG analysis results of $[Re_2(Ile)_4(H_2O)_8](ClO_4)_6$ (Re = Nd, Er) are shown in Figs. 2 and 3, respectively. According to these results, possible mechanisms of decomposition for the two compounds are deduced as follows:

For $[Nd_2(Ile)_4(H_2O)_8](ClO_4)_6$, weight loss was completed in four steps:

$$[Nd_2(Ile)_4(H_2O)_8](ClO_4)_6$$

$$\xrightarrow[9.7\%\ (9.3\%)]{30\text{–}210\,^{\circ}C} [Nd_2(Ile)_4](ClO_4)_6$$

$$\xrightarrow[33.6\%\ (33.7\%)]{210\text{–}273\,^{\circ}C} Nd(ClO_4)_3$$

$$\xrightarrow[12.1\%\ (12.3\%)]{273\text{–}600\,^{\circ}C} NdCl_3 \cdot Nd(ClO_4)_3 \xrightarrow[12.6\%\ (12.4\%)]{600\text{–}950\,^{\circ}C} NdCl_3$$

For $[Er_2(Ile)_4(H_2O)_8](ClO_4)_6$, decomposition was analogous to Nd-complex:

$$[Er_2(Ile)_4(H_2O)_8](ClO_4)_6$$

$$\xrightarrow[7.9\%\ (7.9\%)]{70\text{–}210\,^{\circ}C} [Er_2(Ile)_4H_2O](ClO_4)_6$$

$$\xrightarrow[33.5\%\ (33.5\%)]{210\text{–}297\,^{\circ}C} Er(ClO_4)_3$$

$$\xrightarrow[12.6\%\ (12.4\%)]{297\text{–}600\,^{\circ}C} Er(ClO_4)_3 \cdot ErCl_3$$

$$\xrightarrow[7.5\%\ (8.0\%)]{600\text{–}950\,^{\circ}C} Er(ClO_4)_3 \cdot 5ErCl_3$$

The mass loss (in %) in the brackets are calculated theoretical values of specific forms of product in each step.

Acknowledgements

The authors gratefully acknowledge the National Nature Science Foundation of China for financial support to this work under Grant No. 20073047.

References

[1] H.F. Song, Y. Liu, Chinese Rare Earths 20 (1999) 51.

[2] Y. Kong, Z.C. Li, Z.Z. Liu, T. Pu, J. Southwest China Normal Univ. 24 (1999) 362.

[3] W. Kong, X.Y. Zhang, Microelement Health Study 17 (2000) 67.

[4] Z.Y. Chen, Rural Eco-Environment 15 (1999) 44.

[5] R.Y. Wang, F. Gao, T.Z. Jin, Hua Xue Tong Bao (1996) 14.

[6] J.J. Zhao, W.C. Yang, X.Q. Wang, T.Z. Jin, Polyhedron 14 (1995) 2451.

[7] Z.C. Tan, G.Y. Sun, Y. Sun, A.X. Yin, W.B. Wang, J.C. Ye, L.X. Zhou, J. Therm. Anal. 45 (1995) 59.

[8] D.A. Ditmars, S. Ishihara, S.S. Chang, G. Bernstein, E.D. West, J. Res. Nat. Bur. Stand 87 (1982) 159.